PHYSICAL REVIEW E **84**, 020301(R) (2011)

Elastic weakening of a dense granular pack by acoustic fluidization: Slipping, compaction, and aging

X. Jia,* Th. Brunet,† and J. Laurent

Université Paris-Est, Laboratoire de Physique des Milieux Divisés et Interfaces, CNRS FRE 3300, 5 Boulevard Descartes, F-77454 Marne-la-Vallée, France

(Received 25 January 2011; revised manuscript received 23 July 2011; published 23 August 2011)

Sound velocity measurements in dense glass bead packs reveal significant softening effect at large amplitudes, due to the frictional nonlinearity at the grain contacts. Beyond a certain amplitude, the sound-matter interaction becomes irreversible, leaving the medium in a weakened and slightly compacted state. A slow recovery of the initial elastic modulus is observed after acoustic perturbation, revealing the plastic creep growth of microcontacts. The cross-correlation function of configuration-specific acoustic speckles highlights the relationship between the macroscopic elastic weakening and the local change of the contact networks, induced by strong sound vibration, in the absence of appreciable grain motion.

DOI: 10.1103/PhysRevE.84.020301 PACS number(s): 45.70.−n, 43.35.+d, 91.30.−f

I. INTRODUCTION

A granular medium is an assembly of discrete macroscopic solid grains that interact with each other by dissipative contact forces. Unlike the ordinary solids and liquids, a dense granular medium exhibits multiple metastable configurations and may undergo a transition between solid state to liquid state when a large enough mechanical force is applied by shear or vibration [1–4].

A shaking experiment allows investigation of the complex behavior of driven, athermal granular systems such as compaction, segregation, and pattern formation [1]. In a granular system fluidized by continuous strong vibration where collisions dominate (acceleration normalized with the gravity $\Gamma > 1$), it has been shown [3] that an effective viscosity and effective temperature can be defined in such a granular liquid. By decreasing the amplitude of vibration $\Gamma < 1$, the driven granular medium evolves into an amorphous state [3].

On the opposite side of the liquid-to-solid transition, the jammed granular state is determined by the inhomogeneous contact force networks [1]. A granular solid exhibits very nonlinear dynamics during shearing, accompanied by strong spatial and temporal variations in the contact distribution. In a weakly vibrated granular column, large force variations have been observed on the bottom boundary in the absence of appreciable grain motion, indicating a strong nonlinear and glassy dynamics of the force network [4].

Sound waves propagating through the contact force network provide a natural way to probe accurately and nondestructively the viscoelastic properties of a jammed granular state [5–10]. At large amplitude of vibration, sound waves may serve as controlled perturbation to explore the glassy dynamics of a granular solid [6,7]. Liu and Nagel found previously that sound transmission at $\Gamma \sim 1$ in a glass bead pack under gravity exhibits large temporal fluctuations [6]. Unlike the shaking experiment, such structural relaxation, referred to here as "acoustic fluidization [11]," occurs nevertheless surprisingly where no visible rearrangement of the beads was observed. At moderate vibration ($\Gamma < 0.1$), both a strong hysteretic behavior on the amplitude measurement [6] and a significant modulus softening in the resonance experiment [12] were also observed, but the underlying physics responsible for these nonlinear dynamics still remains unclear on the level of the contacts.

In this paper, we examine quantitatively the hysteretic characteristics of the sound velocity in jammed granular media via pulsed ultrasonic waves. We focus our attention on the irreversible sound-matter interaction in a regime where the grain motion is visibly absent. The resultant rearrangement of the force network is, however, evidenced by the configuration-specific scattered waves. Compared to the previous resonance method (∼150 s), the velocity measurement reported here (∼10 s) is much faster, thus providing an adequate method for highlighting the slow dynamic behavior. All combined measurements, including the packing density, reveal the crucial role of frictional nonlinearity at the grain contact in the elastic weakening and the structural change induced by the acoustic fluidization, and would be helpful for understanding the unjamming or landsliding triggering process [12].

II. EXPERIMENTS

Our granular materials consist of dry polydisperse glass beads of diameter $d = 0.6$–0.8 mm confined in a oedometer cell of 60 mm diam which is filled to a height $H = 20$ mm, with a packing density ≈ 0.61. This type of apparatus allows us to apply a constant uniaxial load P_0 on the bead pack from 85 to 340 kPa. A large longitudinal transducer of 30 mm diam is used as a plane-wave source, transmitting a ten-cycle tone burst centered at low frequency, 50 kHz. The corresponding wavelength λ is ≈ 15 mm, which is much larger than the bead size d, and the coherent wave propagation is detected by another large transducer at the bottom (inset of Fig. 1). To examine the nonlinear response, we vary the input voltage V_{input} from 10 to 250 V, corresponding to a vibration displacement $U \approx 2$–50 nm.

Figure 1(a) shows typical ultrasound transmissions through the bead pack under $P_0 = 340$ kPa for increasing input amplitudes. The absolute value of sound speed c_0 can be measured by the time-of-flight T_0 as $c_0 \approx 770$ m/s. As the input amplitude is increased, we observe that the total transmitted ultrasound is delayed progressively up to ∼2%

*Corresponding author: jia@univ-mlv.fr

†Present address: Université Bordeaux 1, CNRS UMR 5295, F-33405 Talence cedex, France.

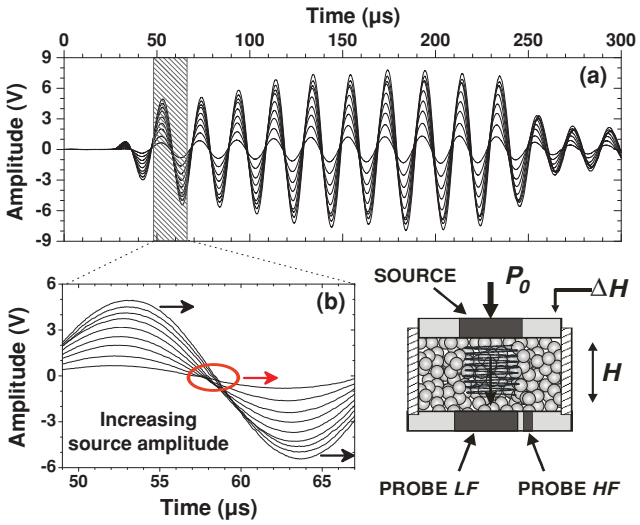

FIG. 1. (Color online) (a) Transmitted ultrasonic wave trains through a glass bead pack under $P_0 = 340$ kPa excited by increasing V_{input}. (b) Progressive delay (closeup). Inset: experimental setup including the source transducer and probes of coherent (LF) and scattered (HF) waves.

[Fig. 1(b)]. Such *softening* effect of sound velocity appears basically different from the usual waveform distortion caused by anharmonicity.

The main investigation is focused on the reversibility of the sound-matter interaction for increasing sound amplitude (Fig. 2); we check if there is any change in the material property and structure after the sound transmission. To do so,

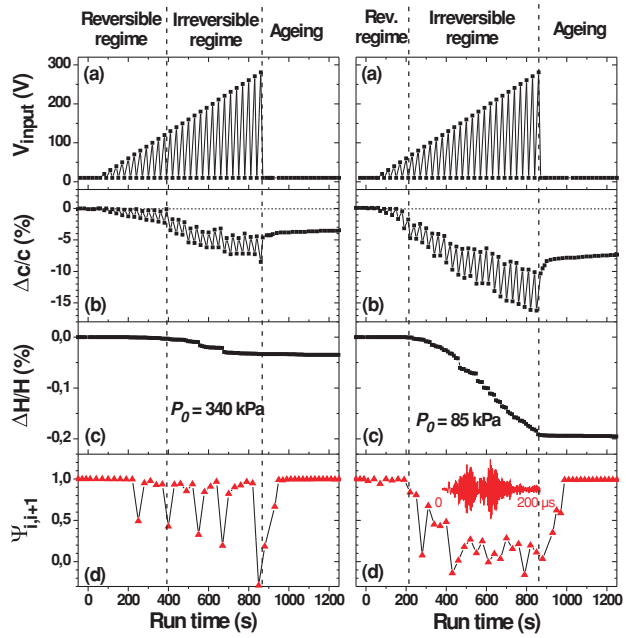

FIG. 2. (Color online) Reversible and irreversible interactions between sound waves and granular packs under $P_0 = 340$ kPa (left) and $P_0 = 85$ kPa (right) versus sound amplitude. (a) Excitation protocol; (b) sound velocity change; (c) packing height variation; (d) resemblance parameter between two successive acoustic speckles. Inset of (d) shows a typical acoustic speckle.

measurements of the wave velocity and the packing density are carried out repeatedly at the lowest input amplitude ($V_{\text{input}} = 10$ V) as a nondisturbing probe, before going up to the next increased amplitude [Figs. 2(a)–2(c)]. In order to monitor the possibly induced rearrangements inside the force networks, we also employ low-amplitude ($V_{\text{input}} = 30$ V), high-frequency ($f = 500$ kHz), multiply scattered waves probed by a pinducer [insets of Figs. 1 and 2(d)]. The structure changes may be evaluated by these configuration-specific acoustic speckles, via the resemblance parameter $\Psi_{i,i+1} = C_{i,i+1}(\tau = 0)/[C_{i,i}(0)C_{i+1,i+1}(0)]^{1/2}$ that was used previously [13]. Here $C_{i,i+1}(\tau)$ with the time lag τ is the cross-correlation function between two successive speckle signals $S_i(t)$ and $S_{i+1}(t)$ recorded every 30 s, before and after the high-amplitude sound transient at low frequency ($f = 50$ kHz).

Roughly, we identify two regimes of fast nonlinear dynamics versus V_{input}. In the first regime, the interaction between sound wave and granular medium is reversible: There is neither velocity change nor sample density variation after the wave passage and the force network remains nearly unchanged, i.e., $\Psi_{i,i+1} \approx 1$, except for a few rare events. In the second regime, however, beyond a certain amplitude threshold depending on the applied load, the sound-matter interaction becomes irreversible. Indeed, the wave velocity and corresponding elastic modulus remain weakened after the wave transient, and slight plastic deformation is also observed corresponding to a compaction of ~ 0.5 μm for one bead layer [Fig. 2(c)]. This characteristic scale associated with our sample compaction is negligibly small compared to those observed in shaking experiments where the rearrangement occurs on the length scale of the grain size d (≈ 0.7 mm). However, the resemblance parameter shows a significant intermittent change in the force networks induced by high-amplitude sound waves, which become much more pronounced and frequent under lower confining pressure [Fig. 2(d)] in conjunction with a more important velocity softening and material compaction [Figs. 2(b)–2(c)]. This finding highlights the relationship between the macroscopic elastic weakening and the local change of the contact network, induced by strong sound vibration in the absence of visible grain motion.

Moreover, we find that there exists a slow dynamics (i.e., aging) in the granular medium, left in a weakened state by the irreversible interaction. The sound velocity slowly returns to its initial value over a number of hours after strong sound transmission [Fig. 2(b)]. This slow recovery, roughly following a logarithmic law, is analogous to the stress relaxation in sheared and compressed granular systems [2] and the aging effect of load-bearing asperities between two rough solids [14] (see next section). During this aging process, the resemblance parameter is close to $\Psi_{i,i+1} \approx 1$, implying that the contact force network remains almost unchanged.

III. MODELING AND DISCUSSION

Let us interpret the sound velocity softening within the framework of the effective medium approach based on contact mechanics. For small-amplitude sound waves propagating in elastic sphere packs under isotropic compression, both compressional and shear velocities c_p and c_s can be derived from the incremental normal and tangential stiffness D_n and

D_t, $c_p \propto [Z(D_n+2D_t/3)]^{1/2}$ and $c_s \propto [Z(D_n+3D_t/2)]^{1/2}$ with Z the coordination number [15]. For large-amplitude sound propagation in the reversible regime $F_t < \mu F_0$, where F_0 and F_t are the normal and tangential forces at the contact and μ the coefficient of friction, two distinct kinds of nonlinear elasticity may come into play between two spheres at large-amplitude vibration [16].

We first consider the nonlinear effects related to the normal force-displacement response. If an oscillating force F_n is applied to two spheres of diameter d initially compressed by a static force F_0, the oscillating displacement U_n can be related to F_n by $F_n \approx D_n U_n(1 + \beta U_n + \delta U_n^2 + \cdots)$. Here D_n is the previously mentioned linear stiffness, $\beta = -1/(4U_0)$ (>0) and $\delta = -1/(24U_0^2)$ (< 0) correspond to the quadratic and cubic nonlinear terms determined by the static compression $U_0 \sim F_0^{2/3}$ (U_0< 0) [12,17]. Accordingly, at large amplitude, we have an associated normal stiffness over one cycle of oscillation $D_n^{NL} \approx D_n(1 + \delta U_n^2)$ and a resultant softening of sound velocity $\Delta c/c \sim \Delta D_n/D_n \sim \delta U_n^2$. Under a pressure P_0($= 4F_0/\pi d^2$) $\approx$100 kPa, the static compression is $U_0 \approx$ –120 nm (the static strain $\varepsilon_0 \sim U_0/d \approx -2\times10^{-4}$) and $\delta \approx -3 \times 10^{-6}$ nm^{-2}. For a sound wave of $U_n \approx$6 nm (the acoustic strain $\varepsilon_a \sim U_n/d \approx 10^{-5}$), the velocity softening due to the Hertz nonlinearity would be only $\Delta c/c \sim$ –0.01%. This mechanism, suggested previously [12], is thus not responsible for the experimental finding (∼–2%).

Let us now examine another mechanism of nonlinearity at the contact, i.e., the hysteretic friction. For two identical spheres, compressed by a constant normal force F_0, an analytical relationship can be derived between the tangential displacement U_t and force F_t, before the sliding threshold (i.e., the Mindlin model) [16]. As depicted in Fig. 3(a), OA and OC represent, respectively, the normalized loading curves for small and large amplitude (U_t^*) of the transverse displacement; AB-BA and CD-DC correspond to the cyclic unloading-reloading curves. For large amplitude of vibration, unloading (U_t^-) and reloading (U_t^+) displacements form a significant hysteresis loop versus F_t (of amplitude F_t^*), implying both the dissipative and the nonlinear elastic features of solid friction. The average stiffness D_t^{NL} corresponds to the slope of the line connecting the end points C and D: $D_t^{NL} < D_t$ when increasing the amplitude U_t^*.

Such softening effect can also be deduced from the elastic response (U_t^E) and the dissipative counterpart (U_t^H) of the hysteretic behavior $U_t(F_t) = U_t^E(F_t) + SU_t^H(F_t)$, as in rocks [18]. Here $U_t^E = (U_t^+ + U_t^-)/2$, $U_t^H = (U_t^+ - U_t^-)/2$, and S is a sign function, $S = 1$ (–1) for F_t increasing (decreasing). For$F_t^* \ll \mu F_0$, we may derive from the Mindlin model (i.e., unloading-reloading) [16],

$$U_t^E(F_t) \approx (2U_0/3)\left(1 + F_t^*/6\mu F_0\right)(F_t/\mu F_0), \quad (1a)$$

$$U_t^H(F_t) \approx (U_0/18)[(F_t/\mu F_0)^2 - (F_t^*/\mu F_0)^2]. \quad (1b)$$

In this work, we are only concerned with the elastic response [Eq. (1a)]; the tangential stiffness is obtained by $D_t^{NL} = (dU_t^E/dF_t)^{-1} \approx D_t(1 - F_t^*/6\mu F_0)$ and consequently $\Delta c/c \sim \Delta D_t/D_t \approx -F_t^*/6\mu F_0 \approx -kU_t^* \sim -\varepsilon_a/\varepsilon_0$. Here $k = [2Ga/3(2-\nu)\mu F_0]$; G and ν are the shear modulus and Poisson ratio of the spheres and a is the radius of the contact area. The experimental data obtained under $P_0 =$ 340 kPa in the reversible regime agree well with such linear decrease of sound velocity [Fig. 3(b)]. Extracting k by the fit and considering the glass bead constants ($G =$ 28 GPa, $\nu = 0.25$) allows us to obtain a friction coefficient $\mu \approx 1.1$, consistent with the previous measurement [10].

To understand the sound-matter interaction in the irreversible regime, we propose the following scenario. At a very large amplitude of vibration, the spheres may slide over each other at the contact when $F_t > \mu F_0$. In a disordered bead pack, such a process is accompanied by the loss of grain contacts, producing the grain rearrangement and significant compaction as in shaking experiments. Our findings on the elastic weakening [Fig. 2(b)] suggest that the irreversible interaction of sound with the granular pack can also take place on a much smaller length scale without the appreciable motion of grains. Indeed, the tiny compaction of tens of microns excludes the rearrangements on the scale of the bead size d. As illustrated in the inset of Fig. 4, the mechanism of sliding between two smooth spheres previously described may take place between the asperities via slipping at large amplitude. For the random height distribution of microasperities [14,16], such slipping may produce the rearrangements of the unstable contacts on the micrometric scale. This picture is consistent with the

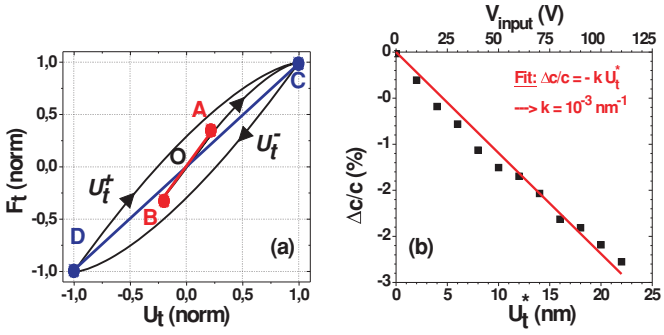

FIG. 3. (Color online) (a) Tangential loading-displacement hysteresis loop: F_t and U_t are normalized by μF_0 and U_t obtained at $F_t = \mu F_0$, respectively. (b) Comparison between measurements and predictions (solid line).

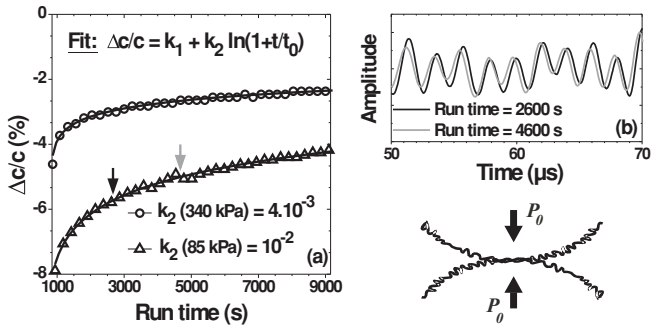

FIG. 4. (a) Slow recovery of sound velocity versus run (waiting) time after large-amplitude sound transmission under $P_0 =$ 340 kPa (circles) and 85 kPa (triangles). Solid lines refer to the fits with the respective k_2. (b) High-frequency acoustic speckles (closeup) recorded at two run times indicated in (a). Inset: squeezed asperities at the bead contact.

observed logarithmic recovery of sound velocity [Fig. 4(a)]. Indeed, as the stiffness D is proportional to the radius $\bar{a}$ of the real contact area ($\Sigma_r \sim \pi \bar{a}^2$), the plastic creep growth of the microcontact $\Sigma_r(t) = \Sigma_{r0}[1 + m \ln(1 + t/t_0)]$ (with m an effective strain-rate sensitivity and t_0 a time constant), weakened or broken by strong vibration, would exhibit a slow recovery of the elastic modulus. The characteristic values $m \approx 4k_2 \sim 10^{-2}$ obtained by fit, are consistent with those found in the literature between rough solid contacts [14]. During this aging or healing regime, the multiply scattered sound waves undergo little modification [Fig. 4(b)], indicating that the spatial distribution of the force chains remains unchanged except for a global enhancement of contacts resulting in the sound velocity increase.

IV. CONCLUSION

We have measured an important softening of sound velocity at large vibration amplitude in jammed granular media (1%–10%). It stems from the nonlinear hysteretic friction at the grain contacts. The sound-matter interaction becomes irreversible beyond a certain amplitude which is stress dependant, weakening the granular medium and causing a tiny compaction. This acoustic fluidization presumably originates from the vibration-induced slipping on the scale of microasperities. Probing simultaneously the contact network changes with the acoustic speckles allows us to evidence a relationship between the global elastic weakening and the local structure relaxation. In addition, we show that during the aging process of the force network, the logarithmic recovery of the elastic modulus is related to the plastic creep growth of broken or weakened contacts but without configuration changes. Our findings might be helpful to highlight the underlying physics of effective granular temperature and particularly the role of noise in the rheology of dense granular flow due to the elastic wave signals propagating away from flips or rearrangement events [19,20].

ACKNOWLEDGMENTS

We thank R. Guyer, P. Johnson, J. Léopoldès, and P. Mills for helpful discussions.

[1] H. M. Jaeger *et al*., Rev. Mod. Phys. **68**, 1259 (1996).
[2] R. R. Hartley and R. P. Behringer, Nature **421**, 928 (2003).
[3] G. D'Anna, P. Mayor, A. Barrat, V. Loreto, and F. Nori, Nature **424**, 909 (2003); G. D'Anna and G. Gremaud, Nature (London) **413**, 407 (2001).
[4] P. Umbanhowar and M. van Hecke, Phys. Rev. E **72**, 030301 (2005).
[5] J. D. Goddard, Proc. R. Soc. London, Ser. A **430**, 105 (1990).
[6] C. H. Liu and S. R. Nagel, Phys. Rev. Lett. **68**, 2301 (1992); Phys. Rev. B **48**, 15646 (1993).
[7] S. Sen *et al*., Phys. Rep. **462**, 21 (2008); S. R. Hostler and C. E. Brennen, Phys. Rev. E **72**, 031303 (2005).
[8] X. Jia, C. Caroli, and B. Velicky, Phys. Rev. Lett. **82**, 1863 (1999); X. Jia, *ibid* **93**, 154303 (2004).
[9] H. A. Makse, N. Gland, D. L. Johnson, and L. Schwartz, Phys. Rev. E **70**, 061302 (2004); L. Bonneau, B. Andreotti, and E. Clement, *ibid*. **75**, 016602 (2007).
[10] Th. Brunet, X. Jia, and P. Mills, Phys. Rev. Lett. **101**, 138001 (2008).
[11] H. J. Melosh, Nature **379**, 601 (1996).
[12] P. Johnson and X. Jia, Nature **437**, 871 (2005).
[13] X. Jia and P. Mills, in *Powders and Grains* (Balkema, Rotterdam, 2001), p. 105; V. Tournat and V. E. Gusev, Phys. Rev. E **80**, 011306 (2009).
[14] T. Baumberger and C. Caroli, Adv. Phys. **55**, 279 (2006).
[15] K. W. Winkler, Geophys. Res. Lett. **10**, 1073 (1983).
[16] K. L. Johnson, *Contact Mechanics* (Cambridge University Press, Cambridge, 1985).
[17] A. N. Norris and D. L. Johnson, J. Appl. Mech. **64**, 39 (1997).
[18] R. A. Guyer, J. TenCate, and P. Johnson, Phys. Rev. Lett. **82**, 3280 (1999).
[19] K. Nichol, A. Zanin, R. Bastien, E. Wandersman, and M. van Hecke, Phys. Rev. Lett. **104**, 078302 (2010).
[20] A. Lemaître and C. Caroli, Phys. Rev. Lett. **103**, 065501 (2009).